

Article

CIPSO-Based Decision Support Method for Collision Avoidance of Super-Large Vessel in Port Waters

Bo Xiang¹ and Yongqiang Zhuo^{2,*}

¹ School of Naval Architecture and Maritime, Zhejiang Ocean University, Zhoushan 316022, China; xiangbo@zjou.edu.cn

² College of Ocean Transportation, Guangzhou Maritime University, Guangzhou 510725, China

* Correspondence: zhuoyq@aliyun.com; Tel.: +86-138-2829-5967

Abstract: Effective and timely collision avoidance decision support is essential for super-large vessels navigating in port waters. To guarantee the navigational safety of super-large vessels, this work proposes a collision avoidance decision support method based on the curve increment strategy with adaptive particle swarm optimization (CIPSO). Firstly, the objective function is constructed based on the multi-objective optimization method. Here, a fuzzy comprehensive evaluation (FCE)-based vessel collision hazard model and vessel speed-varying energy-loss model integrating the Convention on the International Regulations for Preventing Collisions at Sea (COLREGS) are involved. Furthermore, in response to the limitations of the PSO algorithm, which is prone to falling into local optima in the later stages of iteration, a curve increment strategy is incorporated. To improve the performance of the global optimization, it is optimized using a local followed by global search method. The iterative evolution of CIPSO is used to obtain the optimal decision value in the set domain of feasible solutions. Finally, the effectiveness and feasibility of the proposed method are verified by the numerical simulation and large vessel maneuvering simulator, which can provide collision avoidance decision support for ship pilots.

Keywords: super-large vessel; speed-varying collision avoidance; collision avoidance decision support; CIPSO



Citation: Xiang, B.; Zhuo, Y.

CIPSO-Based Decision Support Method for Collision Avoidance of Super-Large Vessel in Port Waters. *Appl. Sci.* **2023**, *13*, 11100. <https://doi.org/10.3390/app131911100>

Academic Editors: Nam-kyun Im, Yong Ma, Qiang Zhang and Guibing Zhu

Received: 2 September 2023

Revised: 30 September 2023

Accepted: 4 October 2023

Published: 9 October 2023



Copyright: © 2023 by the authors. Licensee MDPI, Basel, Switzerland. This article is an open access article distributed under the terms and conditions of the Creative Commons Attribution (CC BY) license (<https://creativecommons.org/licenses/by/4.0/>).

1. Introduction

Along with the relentless development and global expansion of international trade, the shipping industry has assumed paramount significance as an essential and irreplaceable mode of transportation at a global scale. Simultaneously, ship and shipping technologies have undergone rapid and remarkable advancements, characterized by the discernible trend toward the construction of large-scale, high-speed, and specialized vessels [1]. Notably, the emergence of super-large vessels has solidified their position as a principal conduit in the realm of global trade. However, the challenges encountered by super-large vessels while navigating port waters have become increasingly conspicuous. Among these challenges, collision avoidance assumes critical importance. The problem of collision avoidance faced by super-large vessels navigating port waters is marked by distinctive characteristics that set it apart from similar challenges encountered by other vessels. Firstly, the adjustment of course and speed for super-large vessels, owing to their immense size and weight, necessitates a more protracted time frame [2]. Secondly, navigation through narrow waterways and port areas demands a heightened level of dexterity and precision in vessel handling. Lastly, the considerable inertia inherent in super-large vessels results in prolonged stopping or course alteration times, thus necessitating a longer reaction time for executing collision avoidance maneuvers [3]. Consequently, the problem of collision avoidance encountered by super-large vessels operating in port waters has emerged as a field of research deserving of profound attention and scholarly inquiry.

With the development of intelligent algorithms such as Genetic Algorithm (GA) [4], Neural Networks (NNs) [5], Ant Colony Optimization (ACO) [6], and Particle Swarm Optimization (PSO) [7], many experts and scholars have applied heuristic algorithms to the study of vessel collision avoidance issues. Tsou et al. [8,9] used GA to encode four elements, namely, collision avoidance time, collision avoidance steering angle, resumption time, and resumption angle, and evolved them generation by generation through selection, crossover, and mutation operations. The vessel information in the Electronic Chart Display and Information System (ECDIS) was analyzed and processed, i.e., the vessel information in the ECDIS was transformed into a navigational network diagram, and the optimal collision avoidance path was solved using GA. Fiskin et al. [10], Ni et al. [11] Alvarez et al. [12] have also applied GA to this issue.

ACO can provide safety and efficiency collision avoidance decision support for vessel pilots due to the advantages of their distributed computation and positive feedback mechanisms (Lazarowska [13,14]). Tsou and Hsueh [15] proposed an ACO-based collision avoidance path-planning method for vessels. The collision risk between vessels was first converted into the pheromone concentration of each path, and then the best collision avoidance path was gradually determined by simulating ants moving on the path with a high pheromone concentration. Wang et al. [16] proposed a vessel collision avoidance path-planning method considering spatio-temporal interaction effects. By analyzing the spatio-temporal characteristics of vessel movements, an effective path-planning algorithm was designed to avoid vessel collisions. Lyu and Yin [17] proposed an efficient path-planning algorithm that enables autonomous vessels to plan navigational paths quickly and safely in restricted waters. The method combined map data and environmental constraints with an optimization algorithm to achieve an efficient path search and planning. Shen et al. [18] proposed a collision avoidance algorithm for multi-ship systems based on deep reinforcement learning. The best collision avoidance strategy was learned from experience using a deep neural network, and a collision avoidance training method that combines ship maneuvering performance, crew maneuvering characteristics, and consideration of the rules was proposed. Simulation results showed that the algorithm performs better in terms of safety and efficiency than traditional collision avoidance methods.

Hu et al. [19], Xia et al. [20], and Ma et al. [21] have introduced PSO to solve the issue and achieved excellent effects. Zheng et al. [22] proposed a ship collision avoidance method based on an improved cultural particle swarm optimization (CPSO). The CPSO was used to derive the optimal steering angle for ship collision avoidance under the constraints of the rules, and the resulting decision method was finally integrated into electronic nautical charts for validation. The results showed that the method can safely and effectively achieve ship collision avoidance. Compared with other heuristic methods, PSO applied to this issue has the advantages of computational simplicity and fast convergence, which can be used to find the optimal solution for the high-latitude optimization issue in a short period of time [23]. In addition to the above heuristics, many other intelligent evolutionary algorithms have been used in this issue, such as Beetle Antennae Search (BAS) [24], the Danger-Immune Algorithm (DIA) [25], and the Cat-Swarm Biological Algorithm (CSO) [26].

This work compares the above heuristic algorithms when applied to the vessel collision avoidance issue, and analyses these methods item by item, focusing on five aspects: (1) the number of target vessels; (2) the collision avoidance operation of the vessel; (3) the application waters (4) whether the motion or maneuvering characteristics of the vessel are taken into account, classified in terms of high, medium and low; (5) whether the methods comply with the requirements set out in the Convention on the International Regulations for Preventing Collisions at Sea (COLREGS). The comparison results are shown in Table 1.

Table 1. Comparison of vessel collision avoidance methods based on heuristic algorithms.

Methods	Authors	Collision Avoidance Operation	Applied Waters	Motion Characteristics	COLR-EGS
GA	Tsou et al. [8,9]	steering	open water	med	yes
ACO	Lazarowska [13,14]	steering	open water	high	yes
NNs	Shen et al. [18]	steering	open water	high	yes
PSO	Zheng et al. [22]	steering	open water	med	yes
BAS	Xie et al. [24]	steering	open water	med	yes
DIA	Xu [25]	steering	open water	med	yes
CSO	Wei et al. [26]	steering	open water	low	yes

Within the comparative analysis of the aforementioned literature, three primary issues are identified. Firstly, a significant limitation is found in the fact that some studies are geared towards single-vessel collision avoidance, primarily conducting simulation tests for encounter, crossover, and chase-over situations. However, there is still room for improvement in terms of the applicability of multi-vessel collision avoidance. The second predicament pertains to the collision avoidance measures employed in the majority of studies, which primarily focus on steering collision avoidance practices applicable to open-water scenarios. However, the efficacy of these measures in the context of narrow waterways has not been adequately addressed. Lastly, a fundamental concern relates to the alignment with the COLREGS, as well as the consideration of the target vessel's size, type, and maneuvering characteristics. It is important to ascertain the extent to which these factors are taken into account when formulating collision avoidance strategies.

Based on the above issues, an adaptive particle swarm optimization based on a curve increment strategy (CIPSO) for the vessel speed-varying collision avoidance decision method is proposed in this work. Super-large vessels adopt speed-varying collision avoidance measures to ensure navigation safety in the face of multiple vessels encountered during navigation within the port. The method also considers the impact of super-large vessels, deceleration strokes and stroke time on collision avoidance. A vessel collision risk model based on a fuzzy comprehensive evaluation strategy is introduced in this work, wherein COLREGS, navigation safety, and economy are considered to establish a vessel speed-varying energy-loss model. Finally, the CIPSO algorithm is used to find the optimal decision value in the feasible solution domain.

The framework of the decision support method is shown in Figure 1. The navigation of super-large vessels within ports involves the utilization of advanced navigational equipment, such as the Automatic Identification System (AIS), Automatic Radar Plotting Aid (ARPA), and GPS. These tools enable the acquisition of crucial information regarding the vessel's encounters with other target vessels. During this process, the ship's pilot assesses whether an encounter or an emergency situation is unfolding based on the preliminary encounter situation, which relies on the calculated Distance to Closest Point of Approach (d_{CPA}) and Time to Closest Point of Approach (t_{CPA}) (in Section 2.2). In the event of an encounter, the collision risk index (CRI) is determined from the encounter information using the CRI sub-model (in Section 3.1). This sub-model takes into account both the ship domain and maneuvering characteristics of the super-large vessel (in Section 2.1). The encounter situation itself can be divided into two distinct phases: the free action phase and the urgent situation phase. The CRI is compared against a threshold of 0.5 to classify the encounter situation. If the CRI is below 0.5, normal navigation can proceed, and no immediate collision avoidance measures are required. However, ongoing real-time assessment of the encounter situation remains essential. Conversely, if the CRI exceeds 0.5, an urgent situation may arise, necessitating the prompt implementation of appropriate collision avoidance operations. This work introduces a speed-varying collision avoidance decision support model, which combines the CRI sub-model and a speed-varying energy-loss sub-model (in Section 3.3). By incorporating the requirements of COLREGS as constraints for speed-varying collision avoidance, the model ensures that collision avoidance decisions

are both safety-oriented and economically optimal (in Section 3.2). The model function is used as an adaptation of CIPSO (in Section 4). Through an iterative optimization process facilitated by CIPSO, safe speed-varying collision avoidance decision values can be derived. Eventually, collision avoidance decision support can be provided to ship pilots to ensure the safety of super-large vessels navigating in the port.

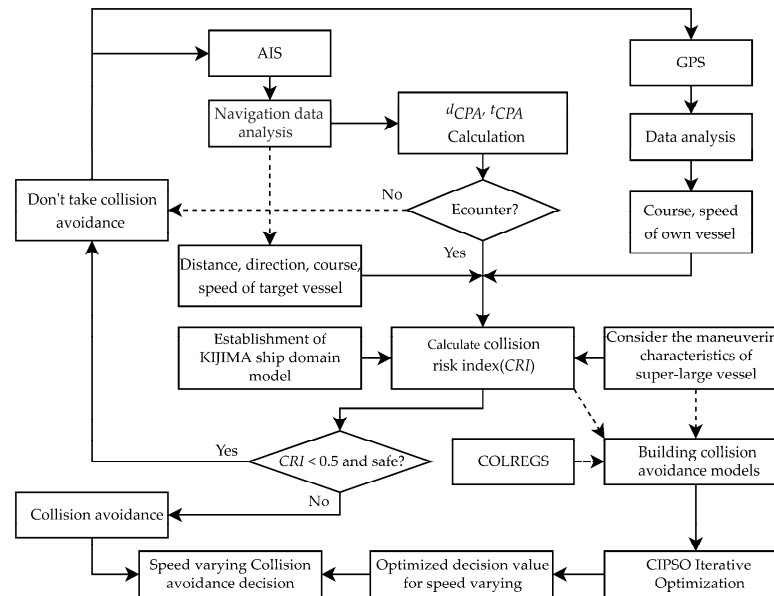


Figure 1. Flowchart of the collision avoidance decision support method.

In conclusion, this work aims to enhance the safety and efficiency of maritime traffic in port waters by providing an effective collision avoidance decision support method that assists port managers and vessel operators in making accurate collision avoidance decisions in complex water environments. The main contributions of this work are as follows:

1. A method is proposed for effective collision avoidance in port waters, considering the maneuvering characteristics and compliance with COLREGS regulations for super-large vessels. The method's suitability and effectiveness are demonstrated in multi-vessel collision avoidance scenarios within ports.
2. A vessel CRI assessment model is developed using the comprehensive judgment theory of fuzzy mathematics. This enables a comprehensive evaluation of multiple factors, including navigational information, deceleration strokes, and stroke time, enhancing risk assessment accuracy for super-large vessels.
3. This work introduces the KIJIMA ship domain model to objectively determine safe encounter distances. This model overcomes the limitations of traditional methods and provides a reliable evaluation of risk severity.
4. PSO is enhanced with a curve increment strategy. This strategy adjusts particle weights dynamically, achieving a balanced exploration of global and local search spaces. The proposed CIPSO algorithm demonstrates faster convergence, improved computational accuracy, and enhanced efficiency, resolving the issue of local optima.

2. Problem Description

Researchers face multiple challenges when studying collision avoidance for super-large vessels proceeding in port waters. Initially, it is imperative to acknowledge the intricacy of the environment surrounding the navigation of a super-large vessel within port waters. Various factors need to be considered, such as port characteristics, vessel characteristics, traffic flow, and weather conditions. The sheer size of a super-large vessel requires special care and coordination to ensure the safety of the vessel. Vessels in port waters have high density, and the risk of collision (CR) between vessels is very high,

requiring effective collision avoidance strategies to reduce risk. In addition, since the control of super-large vessel requires a lot of human and material resources, advanced technologies and methods are needed to improve operational efficiency and reduce human errors.

2.1. Maneuvering Characteristics of Super-Large Vessel in Port Waters

The main navigational characteristics of super-large vessels in port waters include their poor stopping performance, large turning radius, poor maneuvering flexibility, and the influence of external environmental factors such as side wind and cross waves. All these factors increase the CR and grounding of super-large vessels, so special measures and techniques are needed to ensure navigational safety:

- The inertia of the super-large vessel is large and the stopping performance is relatively poor due to its large scale, displacement, and mass;
- The line shape of the super-large vessel is fat and the block coefficient (C_b) is large, although the rudder area coefficient ratio of the vessel is low (generally lower than 1/65), the vessel has good turning and the turning ability index (k) value is large. This means that the scale of water required for a super-large vessel to turn around by itself larger;
- The large inertia and small rudder area coefficient of the super-large vessel make the vessel's sailing stability and turning lag generally poor, i.e., it has a large turning lag index (T) value;
- The quality and size of the super-large vessel make it more susceptible to external environmental factors, such as side winds and cross waves. These factors can cause the vessel to deviate from its intended course and require more time and resources to adjust.

Due to the large tonnage and draft of the super-large vessel, the rudder effect response is slow, and it is difficult to change the course well in a short period of time. Therefore, the speed-varying operation is preferred to avoid collision in port. During speed-varying collision avoidance operations, deceleration is common, and considering the requirements of a "substantial" collision avoidance operation in COLREGS Article 8, deceleration requires a reduce in speed by at least 1/2 [27]. In addition, the speed value cannot be lower than the minimum speed of the vessel to maintain rudder efficiency (except for emergencies). Therefore, COLREGS constrains the range of speed values for speed-varying operations.

2.2. Geometrical Model of Speed-Varying Collision Avoidance for Super-Large Vessels

The geometric model of vessel speed-varying collision avoidance plots the dynamic information of the vessel and the incoming vessel obtained by radar or AIS in the same chart. Plane geometry drawing is used to obtain relevant parameters, determine whether there is a CR, and provide a reference for drivers to take corresponding vessel maneuvering. Let the speed and heading of this vessel be v_0 and C_0 , respectively, the speed and heading of the target vessel be v_1 and C_1 , respectively, the true bearing of the target vessel be T_B , the distance be D , the speed v_{01} , and relative heading C_{01} of this vessel relative to the target vessel. Then, the d_{CPA} and t_{CPA} between vessels can be calculated from the above parameters [28]. The expressions are as follows:

$$d_{CPA} = f_{d_{CPA}}(v_0, C_0, v_1, C_1, D, T_B) \quad (1)$$

$$t_{CPA} = f_{t_{CPA}}(v_0, C_0, v_1, C_1, D, T_B, v_{01}) \quad (2)$$

The vessel slows down to the predetermined speed, requiring a deceleration stroke (D_s) and stroke time (T_s) before slowing down to the predetermined speed. The d_{CPA} value of each target vessel is affected by D_s and T_s . T_s refers to the time required for a vessel to move from the point of loss of control until its inertia disappears. Its size can be calculated according to Equation (3):

$$T_s = -T_{st}(v_t / v_0) \quad (3)$$

D_s refers to the distance traveled by vessel in the direction of vessel speed during the time of impact T_s , which can be estimated by Equation (4):

$$D_s = v_0 T_{st} \left(1 - e^{-T_s / T_{st}} \right) \tag{4}$$

This vessel maintains its course and takes deceleration and collision avoidance operations, assuming the target vessel maintains its course and speed. During the deceleration process, the d_{CPA} values between vessels will continue to change. When the deceleration reaches the predetermined speed v_{0N} , the d_{CPA} will no longer change, and the position of the target vessel relative to the vessel at this time is obtained (x_1, y_1) .

$$\begin{cases} x_1 = D \sin B + v_1 T_s \sin C_1 + D_s \sin(C_0 + 180^\circ) \\ y_1 = D \cos B + v_1 T_s \cos C_1 + D_s \cos(C_0 + 180^\circ) \end{cases} \tag{5}$$

Then, we can obtain the new distance D_N of the target vessel

$$D_N = \sqrt{(x_1)^2 + (y_1)^2} \tag{6}$$

The velocity components of the vessel's speed on the x and y axes are:

$$\begin{cases} v_{x_0} = v_{0N} \sin C_0 \\ v_{y_0} = v_{0N} \cos C_0 \end{cases} \tag{7}$$

The velocity components of the target vessel's speed on the x and y axes are:

$$\begin{cases} v_{x_1} = v_1 \sin C_1 \\ v_{y_1} = v_1 \cos C_1 \end{cases} \tag{8}$$

The velocity components of the relative speed of two vessels on the x and y axes are:

$$\begin{cases} v_{x_{01}} = v_{x_1} - v_{x_0} \\ v_{y_{01}} = v_{y_1} - v_{y_0} \end{cases} \tag{9}$$

The relative speed of the two vessels v_{01N} is:

$$v_{01N} = \sqrt{v_{x_{01}}^2 + v_{y_{01}}^2} \tag{10}$$

The relative heading of the two vessels C_{01N} is:

$$C_{01N} = \begin{cases} \arctan(v_{y_{01}} / v_{x_{01}}) & v_{x_{01}} \geq 0, v_{y_{01}} \geq 0 \\ 90^\circ & v_{x_{01}} \geq 0, v_{y_{01}} = 0 \\ 180^\circ + \arctan(v_{y_{01}} / v_{x_{01}}) & v_{y_{01}} < 0 \\ 270^\circ & v_{x_{01}} < 0, v_{y_{01}} = 0 \\ 360^\circ + \arctan(v_{y_{01}} / v_{x_{01}}) & v_{x_{01}} < 0, v_{y_{01}} < 0 \end{cases} \tag{11}$$

The true orientation of the target vessel T_{BN} is:

$$T_{BN} = \begin{cases} \arctan(x_1 / y_1) & y_1 > 0 \\ 180^\circ + \arctan(x_1 / y_1) & y_1 < 0 \\ 0^\circ & y_1 = 0, x_1 = 0 \\ 90^\circ & y_1 = 0, x_1 > 0 \\ 270^\circ & y_1 = 0, x_1 < 0 \end{cases} \tag{12}$$

d_{CPA1} and t_{CPA1} after deceleration are denoted as:

$$\begin{cases} d_{CPA1} = D_N \sin(C_{01N} - T_{BN} - 180^\circ) \\ t_{CPA1} = D_N \cos(C_{01N} - T_{BN} - 180^\circ) / v_{01N} \end{cases} \quad (13)$$

3. Super-Large Vessel Collision Avoidance Model

3.1. CRI Objective Function Model

CRI is a fuzzy concept that measures the degree of collision risk between vessels. The $CRI \in [0,1]$, specifically, $CRI = 0$ indicates that there is no CR between vessels, and the vessel can continue sailing in its current state; $0 < CRI < 1$ indicates that there is a CR between vessels [29]. By setting a safety threshold, it can be divided into several levels, such as “low risk”, “moderate risk”, and “high risk”, and appropriate avoidance operations can be undertaken based on this. $CRI = 1$ indicates that the vessel has entered an emergency, and relying solely on the vessel’s avoidance operation will not avoid collision with the target vessel. The main way to determine whether there is a CR between vessels is to comprehensively analyze the distance D and relative orientation between the two vessels θ , vessel speed ratio K , nearest encounter distance d_{CPA} , recent meeting time t_{CPA} , Li et al. [30] used the above five elements as basic evaluation parameters and quantitatively analyzed the vessel risk model using the fuzzy comprehensive evaluation method based on fuzzy mathematics.

Considering the five factors that affect the risk of vessel collision, establish a target factor set:

$$U = \{D, \theta, K, d_{CPA}, t_{CPA}\} \quad (14)$$

Establish a comment set:

$$V = \{u_1, u_2\} \quad (15)$$

where u_1 indicates danger; u_2 indicates security.

W is the weight matrix of influencing factors:

$$W = (w_D, w_\theta, w_K, w_{d_{CPA}}, w_{t_{CPA}}) = (0.14, 0.10, 0.08, 0.36, 0.32) \quad (16)$$

Establish an evaluation matrix:

$$r = \begin{pmatrix} u_D & 1 - u_D \\ u_\theta & 1 - u_\theta \\ u_K & 1 - u_K \\ u_{d_{CPA}} & 1 - u_{d_{CPA}} \\ u_{t_{CPA}} & 1 - u_{t_{CPA}} \end{pmatrix} \quad (17)$$

where $r_D, r_\theta, r_K, r_{d_{CPA}}$ and $r_{t_{CPA}}$ represent risk membership for each influencing factor; the range of values is $[0,1]$.

$$u_D = \begin{cases} 1 & 0 \leq D \leq D_1 \\ \left(\frac{D_2 - D}{D_2 - D_1}\right)^2 & D_1 < D \leq D_2 \\ 0 & D > D_2 \end{cases} \quad (18)$$

$$u_\theta = 1/2 \left(\cos(\theta - 19) + \sqrt{400/289 + \cos^2(\theta - 19)} \right) - 5/17 \quad (19)$$

$$u_K = 1 / \left(1 + k_w / K \sqrt{K^2 + 1 + 2K \sin C} \right) \quad (20)$$

where C is the collision angle between two vessels, k_w is a constant taken as 2, $D_1 = K_1 K_2 K_3 D_{LA}$, and D_{LA} is the distance of the last-minute action, whose value is generally taken as 12 times the vessel’s length [31]. $D_2 = K_1 K_2 K_3 R$; the value of K_1 depends on the visibility, the value of K_2 depends on the waters in which the vessel is navigating, and the

value of K_3 depends on the human factor. R is the radius of the dynamic boundary area of this vessel.

$$R = 1.7\cos(\theta - 19) + \sqrt{4.4 + 2.89\cos^2(\theta - 19)} \tag{21}$$

$$r_{d_{CPA}} = \begin{cases} 1 & 0 \leq d_{CPA} \leq d_1 \\ 1/2 - 1/2\sin(180^\circ / (d_2 - d_1)(d_{CPA} - (d_2 - d_1)/2)) & d_1 \leq d_{CPA} \leq d_2 \\ 0 & d_{CPA} \geq d_2 \end{cases} \tag{22}$$

where d_1 is the vessel’s safe encounter distance and d_2 is the absolute safe encounter distance; generally, take $d_2 = 2d_1$.

In the traditional method of determining the safe encounter distance of vessels, a fixed threshold is mainly set. There may be a greater CR when the distance between vessels is less than this determined threshold, but the accuracy of this method can be limited due to the complexity and dynamics of vessel movements in ports. Incorporating a ship domain model can improve the accuracy of encounter distance calculations by more accurately simulating vessel motion and behavior and considering factors such as vessel size, shape, draft, speed, and maneuvering. The ship domain is a water area around the vessel that exists to avoid collision accidents and ensure the safety of vessel navigation, and its size is affected by a variety of factors, such as the size of the vessel, speed and angle of encounter, and visibility of the water [32].

Since the inception of the elliptical ship domain concept established by FUJII [33], numerous experts and scholars worldwide have conducted relevant research in the ship domain model, establishing various ship domain models of different shapes and applying them to domains such as maritime traffic risk assessment, collision avoidance, and waterway traffic planning. These models include the sector model for open water proposed by GOODWIN [34], the circular model with center offset proposed by DAVIS et al. [35], the elliptical model proposed by COLDWELL [36] and KIJIMA et al. [37], and the azimuthal octagonal model proposed by PIETRZYKOWSKI et al. [38]. Wang et al. [39] classified these into three types of ship domain model, such as circular, elliptical, and polygonal, based on which corresponding mathematical models were established for simulation and analysis. The results indicate that the DAVIS and PIETRZYKOWSKI models are suitable for risk assessment in maritime traffic, while the FUJII, GOODWIN, COLDWELL, and KIJIMA models are suitable for collision avoidance. In practical applications, the use of the GOODWIN or KIJIMA models is safer than use of the COLDWELL and FUJII models. Although the GOODWIN model considers the different safe encounter distances of vessels in different encounter scenarios, it is a static model related only to the length of the vessel. In contrast, the KIJIMA model is influenced by multiple parameters, such as vessel length, width, course, and speed, and is a dynamic domain model that comprehensively considers vessel scale and encounter situations, better reflecting the characteristic differences of the vessel’s safe encounter distances in different scenarios.

The KIJIMA model consists of two parts: watching and blocking areas. The watching area is a section of the vessel in the forward direction, which is used to detect the obstacles in front of the vessel. The length of the watching area can be set according to the actual situation, which usually depends on the vessel’s speed and reaction time and other factors. The blocking area refers to some area around the ship, which describes a situation in which the vessel is blocked during movement. The blocking area is calculated based on information such as the location and size of obstacles detected in the watching area. Figure 2 shows that the KIJIMA model is an approximate ellipse shape, consisting of two differently shaped semi-ellipses at the top and bottom. They share the half-axis S_b in the forward transverse direction of the vessel, while the lengths of the half-axes R_{bf} and R_{bt} in the bow and transom directions are different. In addition, the lengths of all the semi-axes change

dynamically with the vessel’s speed and parameters such as the encounter situation to adapt to different sailing situations and environmental conditions.

$$\begin{cases} R_{bf} = L + (1 + s)T_{90}v_0 \\ R_{ba} = L + T_{90}v_0 \\ S_b = B + (1 + t)D_T \end{cases} \quad (23)$$

$$T_{90} = 0.67/v_0\sqrt{A_D^2 + (D_T / 2)^2} \quad (24)$$

$$\begin{cases} A_D = Le^{0.3591\log v_0 + 0.0952} \\ D_T = Le^{0.5441\log v_0 - 0.0795} \end{cases} \quad (25)$$

$$\begin{cases} s = 2 - (v_0 - v_1) / v_0, t = 1 & \text{Headon} \\ s = 2 - \alpha / 180^\circ, t = \alpha / 180^\circ & \text{Crossing} \\ s = 1, t = 1 & \text{Overtaking} \end{cases} \quad (26)$$

$$\alpha = |180^\circ - \langle v_0, v_1 \rangle| \quad (27)$$

where, in (23)–(27), the x -axis represents the vessel’s bow direction and the y -axis represents the vessel’s positive transverse direction; L and B are the length and breadth of the vessel, respectively; v_0 and v_1 are the speeds of the vessel and the target vessel, respectively; T_{90} is the time required for the vessel to steer at 90° ; A_D and D_T are the inlet and initial diameter of the corresponding vessel’s gyrations, respectively; s and t are the influence coefficients of the vessel’s domain in different encounter situations; α is the complementary angle to the angle of the heading line between vessels.

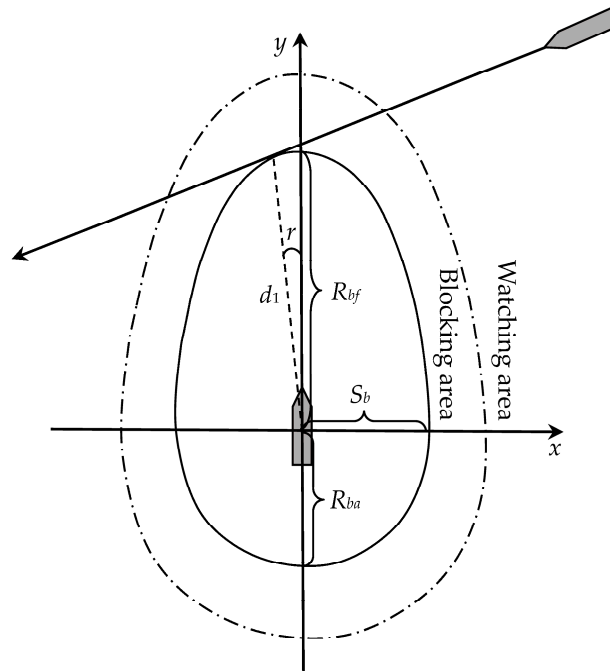


Figure 2. KIJIMA ship domain model.

The safe encounter distance d_1 (within the blocking area, the intrusion of other vessels is rejected, and the intrusion is regarded as $r_{d_{CPA}} = 1$, where d_1 is taken as the boundary of the blocking area of the vessel’s domain) and the safe passage distance d_2 (the vessel does not empirically consider collision avoidance operation when $D \geq 2d_1$, i.e., $r_{d_{CPA}} = 0$)

were obtained based on the KIJIMA model. This work is based on the ellipse origin to edge distance equation:

$$d = \sqrt{a^2b^2 / (a^2\sin r^2 + a^2\cos r^2)} \tag{28}$$

where a is the long half-axis of the ellipse, b is the short half-axis of the ellipse, and r is the angle with the long half-axis a .

Derive the formula for d_1 :

$$d_1 = \begin{cases} \sqrt{R_{bf}^2 S_b^2 / (R_{bf}^2 \sin r_1^2 + S_b^2 \cos r_1^2)} & y \geq 0 \\ \sqrt{R_{ba}^2 S_b^2 / (R_{ba}^2 \sin r_2^2 + S_b^2 \cos r_2^2)} & y < 0 \end{cases} \tag{29}$$

where (x, y) are the coordinates of the closest point of approach in the coordinate system established in the ship domain; r_1, r_2 are the angles between the line from the vessel to the closest point of approach and R_{bf}, R_{ba} , respectively.

$$r_{t_{CPA}} = \begin{cases} 1 & 0 \leq t_{CPA} \leq t_1 \\ \left(\frac{t_2 - t_{CPA}}{t_2 - t_1}\right)^2 & t_1 < t_{CPA} \leq t_2 \\ 0 & t_{CPA} \geq t_2 \end{cases} \tag{30}$$

$$t_1 = \begin{cases} \sqrt{D_1^2 - d_{CPA}^2} / v_{01} & d_{CPA} \leq D_1 \\ (D_1 - d_{CPA}) / v_{01} & d_{CPA} \geq D_1 \end{cases} \tag{31}$$

$$t_2 = \sqrt{D_2^2 - d_{CPA}^2} / v_{01} \tag{32}$$

$$CRI = w_D u_D + w_\theta u_\theta + w_K u_K + w_{d_{CPA}} u_{d_{CPA}} + w_{t_{CPA}} u_{t_{CPA}} \tag{33}$$

Build a collision risk objective function as follows:

$$f_1(x_i) = \max_{1 \leq i \leq N} f_i(u_D, u_\theta, u_K, u_{d_{CPA}}, u_{t_{CPA}}) \tag{34}$$

where $f_1(x_i)$ is the collision risk between the i -th target vessel and the vessel, $f_1(x_i) \in [0,1]$; N is the number of target vessels, and the smaller the objective function value, the lower the collision risk.

3.2. Speed-Varying Energy-Loss Function Model

The deceleration and collision avoidance operation of the vessel is subject to the constraints of the COLREGS, and the speed range of the vessel should be between the minimum speed v_{se} and the initial speed v_0 that maintains the steering effect, which means that the feasible solution domain for vessel deceleration and collision avoidance is $[v_{se}, v_0/2]$. The bigger the deceleration of a vessel, the greater the loss in the vessel's energy consumption when restoring speed. Therefore, the speed of the vessel after a speed reduction should be as large as possible within the limited range, and the speed-varying energy loss function f_2 should be taken as:

$$f_2(x_i) = \frac{x_i - v_0 / 2}{v_{se} - v_0 / 2} \tag{35}$$

where $f_2(x_i)$ is the value range of $[0,1]$, and the smaller the value, the greater x_i and the higher the value of i .

3.3. Total Objective Function Model

The value range of the collision risk function and constructed speed-varying energy-loss function is between 0 and 1, and the smaller the value of the function, the better the effect of speed-varying collision avoidance. To facilitate the search for the optimal value of the objective function, certain weights can be assigned to each of the above two sub-objective functions. Thus, the super-large vessel speed-varying collision avoidance model can be optimized accordingly.

$$f(x_i) = \alpha f_1(x_i) + \beta f_2(x_i) \quad (36)$$

where x_i is the vessel speed value of individual i -th in the population of the CIPSO algorithm; α and β are weight coefficients with $\alpha + \beta = 1$. The assignment of weights to α and β should be determined through experimental tests.

4. Collision Avoidance Decision Support Based on CIPSO Algorithm

4.1. Basic Principles of PSO

Assume that the total number of particles in a D -dimensional search space is N , where the i -th particle is represented as a D -dimensional vector $X_i = (x_{i1}, x_{i2}, \dots, x_{iD})$, $i = 1, 2, \dots, N$. The flight speed of the i -th particle is also a D -dimensional vector, denoted as $V_i = (v_{i1}, v_{i2}, \dots, v_{iD})$, $i = 1, 2, \dots, N$. The individual extreme value found before the i -th particle is denoted as $P_{best} = (P_{i1}, P_{i2}, \dots, P_{iD})$, $i = 1, 2, \dots, N$. The global extremum of particle swarm is denoted as $g_{best} = (g_1, g_2, \dots, g_D)$. In the elementary particle swarm, particles update their speed and position according to the following formula:

$$v_{ij}(t+1) = wv_{ij}(t) + c_1r_1(t)[P_{ij}(t) - x_{ij}(t)] + c_2r_2(t)[P_{gj}(t) - x_{ij}(t)] \quad (37)$$

$$x_{ij}(t+1) = x_{ij}(t) + v_{ij}(t+1) \quad (38)$$

where c_1 and c_2 are acceleration factors; r_1 and r_2 are a uniform random number of [0,1]. The first part of Equation (37) represents the speed of particles before each update, which is used to ensure the algorithm's global convergence. The second and third parts provide the algorithm with a local convergence ability. The inertia weight value w represents the degree of inheritance of the original speed.

4.2. CIPSO Algorithm

In the PSO, the inertia weight controls the speed and direction of the particles moving in the search space. If the inertia weight is excessively large, the particles may skip the global optimal solution and fall into the local optimal solution. Conversely, if the inertia weight is excessively small, particles may persistently meander around the local optimal solution and find it difficult to jump out. By dynamically adjusting the inertia weights, the curve-increasing strategy can gradually increase the inertia weights when the individual optimal value of the particle continuously decreases, thus prompting the particle to jump out of the local optimal solution and move toward the global optimal solution. When the particle approaches the global optimal solution, the inertia weight will gradually decrease, thus enabling the particle to search repeatedly near the local optimal solution and improving the search accuracy of the algorithm. Therefore, the curve-increasing strategy can help the PSO to avoid falling into the local optimal solution too early, while maintaining a balance between global search and local search, thus improving the algorithm's search efficiency and convergence accuracy.

Curve increasing is a control strategy based on the exponential function image proposed in this work, as shown in Figure 3, which tends to become smoother as the independent variable increases. Given the value of inertia weight w_{max} , the curve-increasing formula is:

$$w_1 = w_{max} - (w_{max}/T_{max})t_{(time)} \quad (39)$$

$$w = e^{-w_1} \tag{40}$$

where w_{max} is the set of larger inertia weights ($w_{max} \geq 1$), $t_{(time)}$ is the number of current iterations, and the maximum number of iterations is T_{max} ; as the number of iterations increases, w_1 gradually decreases and w gradually increases. Using the above adaptive weight-change formula, the particle has a fine search ability in the early stage due to the small weight value and, combined with the image, it can be seen that the algorithm iterates the early w_1 value in a large reduction trend range. This is extremely slow, ensuring the adequacy of the particle local search, and the later change trend gradually increases, causing a certain perturbation effect on several local solutions and ensuring that a global search is possible. w_{max} value late trend changes occur; the purpose of these is no longer to ensure faster convergence in the conventional sense, as the trend of change is actually relatively steep and absolutely smooth after the two transformations of Equations (39) and (40).

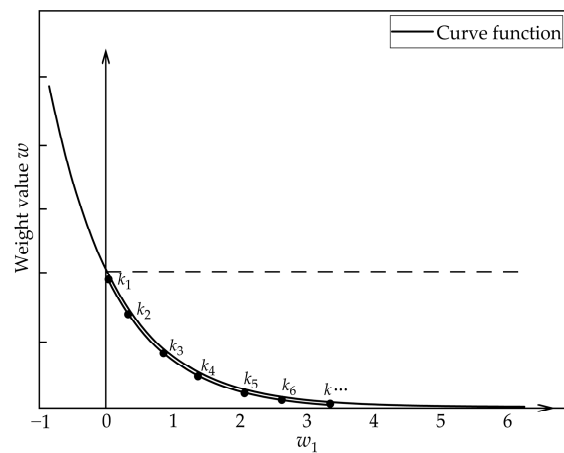


Figure 3. Curve incremental strategy function.

Regarding the acceleration factor, this work proposes an improved second-order oscillation method, which introduces a curve-increasing strategy that combines two populations to improve the diversity of the population and further improve the global search ability of the algorithm. The improved formula is as follows:

$$v_{ij}(t) = e^{-w_1} v_{ij}(t) + r_1 [P_{ij}(t) - (1 + \mu_1)x_{ij}(t) + \mu_1 x_{ij}^*(t)] + r_2 [P_{gi}(t) - (1 + \mu_2)x_{ij}(t) + \mu_2 x_{ij}^*(t)] \tag{41}$$

$$x_{ij}^*(t) = x_{ij}(t)$$

$$x_{ij}(t + 1) = x_{ij}(t) + v_{ij}(t + 1)$$

where x_{ij}^* is a new species group; T is the current iteration number; second-order oscillation factor $\mu_{1,2}$ is denoted as

$$\mu_1 = (2\sqrt{c_1 rand() - 1}) \cdot rand() \cdot rand() / c_1 \quad w < 2/3w_{max} \tag{42}$$

$$\mu_1 = (2\sqrt{c_1 rand() - 1}) \cdot rand() \cdot (1 + rand()) / c_1 \quad w \geq 2/3w_{max} \tag{43}$$

where c_1 and c_2 are an artificially set acceleration factor; $rand()$ is a random number from 0 to 1. The optimization process of the CIPSO algorithm is shown in Figure 4.

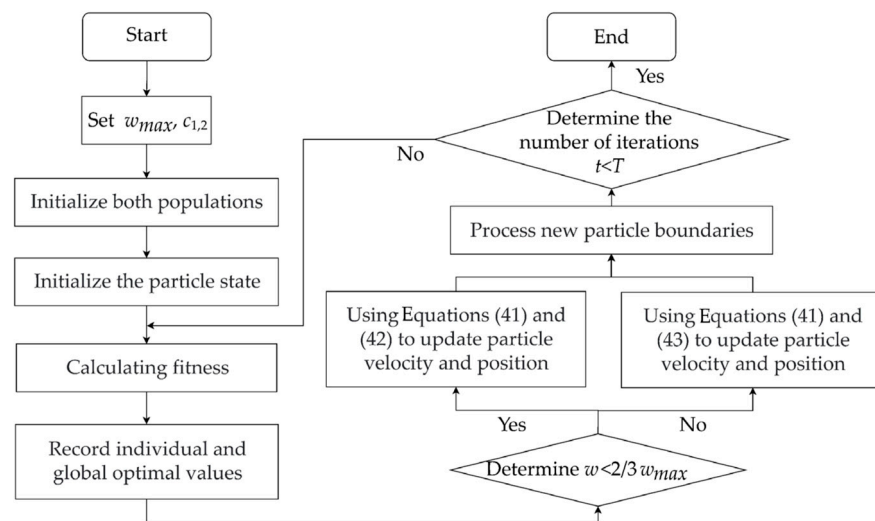


Figure 4. Optimization steps of CIPSO algorithm.

Finally, to further understand the solution process of the CIPSO algorithm, the pseudo-code of Algorithm 1 is presented.

Algorithm 1: Pseudo code of CIPSO algorithm.

```

1  FOR each particle ( $i$ )
2    Set up parameters ( $w_{max}, c_1, c_2$ )
3    Initialize particle position ( $x_{ij}$ ) randomly within the permissible range
4    Initialize particle velocity ( $v_{ij}$ ) randomly within the permissible range
5    Initialize the particle's best position ( $P_{best}$ )
6    IF the particle's fitness value is better than the global best fitness value ( $g_{best}$ )
7      Update global best position ( $g_{best}$ )
8    END
9  END
10 Iteration  $t = 1$ 
11 DO
12  FOR each particle ( $i$ )
13    Calculate inertia weight ( $w$ ) according to Equations (39) and (40)
14    Calculate second-order oscillation factor ( $\mu_1, \mu_2$ ) according to Equations (42) and (43)
15    Update particle velocity and particle position according to Equation (41)
16    Calculate fitness value
17  IF the particle's fitness value is better than its best fitness value ( $P_{best}$ )
18    Update the particle's best position ( $P_{best}$ )
19  END
20  IF the particle's fitness value is better than the global best fitness value ( $g_{best}$ )
21    Update global best position ( $g_{best}$ )
22  END
23   $t = t + 1$ 
24  WHILE maximum iteration or minimum error criteria are not attained
  
```

5. Simulation Analysis

5.1. Method Validation

To validate the proposed speed-varying collision avoidance method for super-large vessels, a simulator was selected to conduct single-vessel collision avoidance experiments in this work. Speed-varying collision avoidance and steering collision avoidance were used for simulations. The data were compared and analyzed from the perspectives of CR, and changes in d_{CPA} and t_{CPA} values. According to rule 8 of COLREGS, the vessel needs to undertake substantial collision avoidance operations. After several simulator experiments, it was decided to set the steering collision avoidance angle to 30° in the

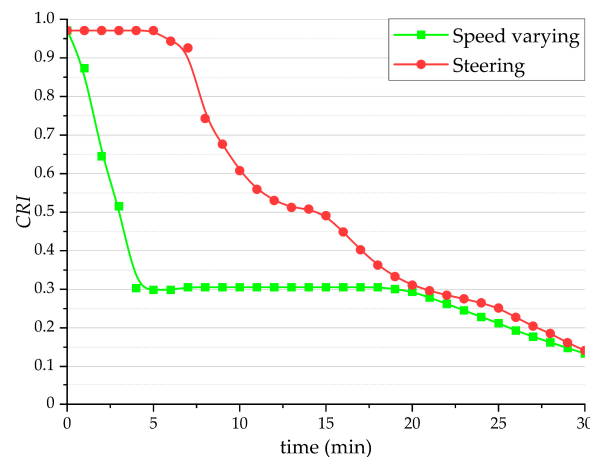


Figure 6. Comparison of the change in the CRI of TG relative to OS in two collision avoidance operations.

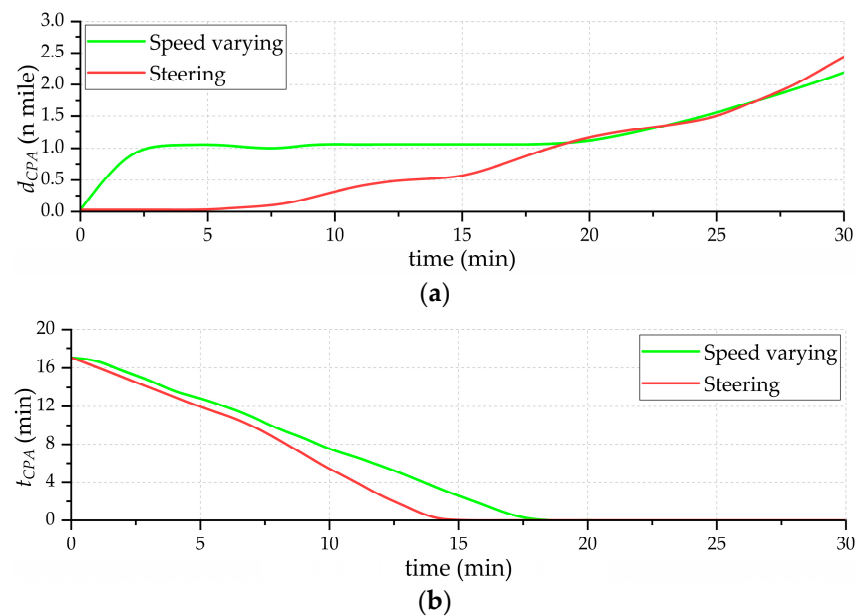


Figure 7. Comparison of d_{CPA} and t_{CPA} value changes between TG and OS in two collision avoidance operations. (a) The change of d_{CPA} value; (b) The change of t_{CPA} value.

5.2. Method Application

To verify the feasibility and effectiveness of the decision support method, a case study of multiple vessels encountered in the port is selected. The vessel (OS) is 290.5 m in length (L) and 50 m in breadth (B), has a deadweight weight of 202,000 tons, a heading of $C_0 = 330^\circ$, a speed of $v_0 = 13$ knots, and a minimum speed of $v_{se} = 2$ knots to maintain rudder effectiveness. The vessel was navigating normally in a port area with good visibility, and the ship pilots had excellent seamanship. At the same time, three vessels (numbered TG1–TG3) were encountered and were not in mutual view. The information regarding the encounter situation of each target vessel, obtained through radar plotting and AIS, is presented in Table 2. Here, a positive value of d_{CPA} indicates that TG passed through the bow of OS, while a negative value indicates passing through the stern of OS.

In Table 2, it can be seen that if all four vessels comply with COLREGS, the safe encounter distance (d_1) is calculated to be 1.0463 n miles and the distance between the vessel and TG1, TG2, and TG3 is less than d_1 ; then, OS needs to give way to all TGs. Priority should be given to avoiding the TG1 with the shortest t_{CPA} , and the OS should adopt a reverse-deceleration collision avoidance method.

Table 2. Target vessels encounter situational parameters.

Target Vessel	TG1	TG2	TG3
Vessel type	Fish boat	LNG	Bulk carrier
Course (°)	90.0	253.0	93.0
Direction (°)	313.5	008.4	307.8
Speed (knot)	7	9	9
Distance (n mile)	3.561	4.522	5.483
d_{CPA} (n mile)	0.242	0.075	0.080
t_{CPA} (min)	12.13	19.32	16.93
Displacement (t)	286.0	89,634.0	23,565.0
Length (m)	24.4	274.3	182.9
Breadth (m)	7.2	43.3	22.6

Model parameter settings: By analyzing the navigational environment and human factors of the case, the values of K_1 , K_2 and K_3 are taken as 1, 2 and 1, respectively. Following several iterations of the optimization algorithm, the final test resulted in an optimal weight assignment of $\alpha = 0.8$, $\beta = 0.2$. To verify the superiority of the proposed CIPSO algorithm, three classical intelligent algorithms were selected for comparison experiments: Simulated Annealing Algorithm (SA), GA, and PSO. The population size in all algorithms was set to 100 and the maximum number of iterations was set to 300. Parameter settings in SA were as follows: the initial temperature was set to 100°, and the temperature decay coefficient was set to 0.95 [40]. Parameter settings in GA were as follows: the crossover probability was 0.8, and the variance probability was 0.05 [41]. Parameter settings in CIPSO were as follows: the update speed limit range of particles was $[-1.5, 1.5]$, w_{max} was set to 1.2, and the individual position (vessel speed) constraint was set to $[v_{se}, v_0/2]$, that is, $[2, 6.5]$. The particle inertia weight w of the PSO algorithm was set to 0.9, the acceleration factors c_1 and c_2 were set to 2 [42], and other parameter settings were the same as CIPSO.

Result analysis: Figure 8 shows the iteration process and convergence results of each algorithm. It is observed that the CIPSO algorithm converges faster and stabilizes around the 23rd generation, and the standard PSO algorithm only stabilizes around the 41st generation. However, the GA algorithm and SA algorithm only stabilized in the 35th and 59th generations, respectively, and did not find the optimal solution within the set number of iterations, so the accuracy of these algorithms remains to be discussed. The CIPSO algorithm takes 5–10 s to execute, which can ensure the real-time collision avoidance decision. This indicates that the curve incremental strategy adopted in this work can effectively adjust the behavior of the particles, enabling the algorithm to better balance the relationship between global and local searches, thus improving the search efficiency and convergence accuracy of the algorithm.

The CIPSO algorithm calculated the optimal value as (3.7372, 0.345644), which means this vessel’s optimal collision avoidance operation requires it to slow down to 3.7372 knots. The vessel decelerated from 13 knots to 3.7 knots, with a reverse deceleration stroke of 1.04 n miles and a stroke time of 8.3 min. After stabilizing to 3.7 knots, the d_{CPA} values with TG1, TG2, and TG3 were [1.10, 2.57, 1.54], the d_{CPA} values between OS and each TG were greater than the set d_1 value, and the OS could safely navigate the port, avoiding all vessels. Figure 9 shows the change curve of collision risk when the vessel undertakes the deceleration collision avoidance operation; the CRI value of each TG relative to OS is gradually reduced to below 0.3 within 10 min, which reduces the CR.

Figure 10 shows the change in the distance between each TG and OS during the collision avoidance process, and the encounter distance between each TG and OS is higher than d_1 . The value of the closest encounter distance between TG1 and OS is very similar to the value of d_1 , which also indicates that the speed value given by the speed-varying collision avoidance decision makes the energy loss of the vessel as small as possible, and simultaneously maximizes the safety of the vessel’s encounter. The above analysis can

conclude that the speed-varying collision avoidance decision is effective and can feasibly safely avoid all target vessels.

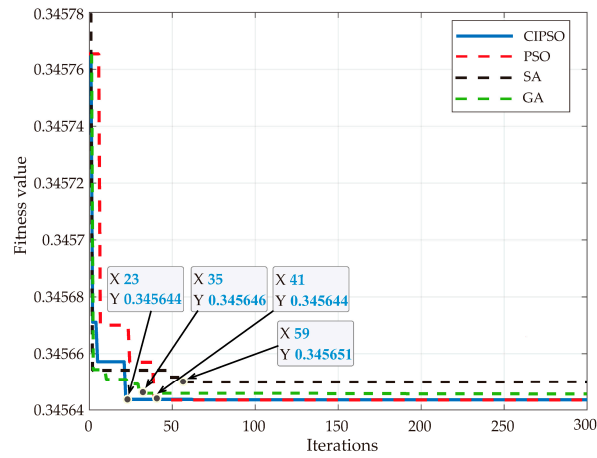


Figure 8. Comparison diagram of fitness changes.

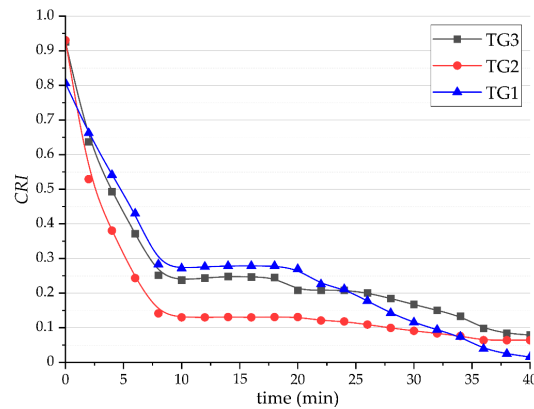


Figure 9. Change curve of CRI in the collision avoidance process.

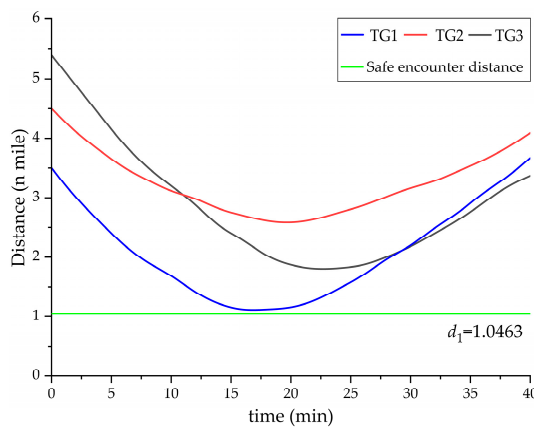


Figure 10. Change the curve of encounter distance between OS and each TG.

To further validate the feasibility and effectiveness of the method, a large-vessel maneuvering simulator was used to conduct multi-vessel simulation experiments. Figure 11 shows the trajectory generated after manipulating collision avoidance in the simulation case in the simulator. In the figure, the green vessel (OS) is the simulated vessel, while the other vessels (TG1, TG2, TG3) are the simulated target vessels. The virtual shadow of the vessel represents the position of the vessel at a certain time. The numbers in the

figure represent different time points, with 1 being the starting time point, and a time interval of 4 min. From Figure 11, it can be seen that the distance between the trajectories of OS is equal at the third moment, indicating that OS is reversing and decelerating to the predetermined safe speed. At the fourth moment, the TG1 has safely passed the bow of the OS and is a long, safe distance from the OS. At the sixth moment, TG2 and TG3 are also sailing in their respective directions past the bow of the OS. This indicates that the safe speed provided by this decision support method meets the safety requirements of super-large vessel navigation.

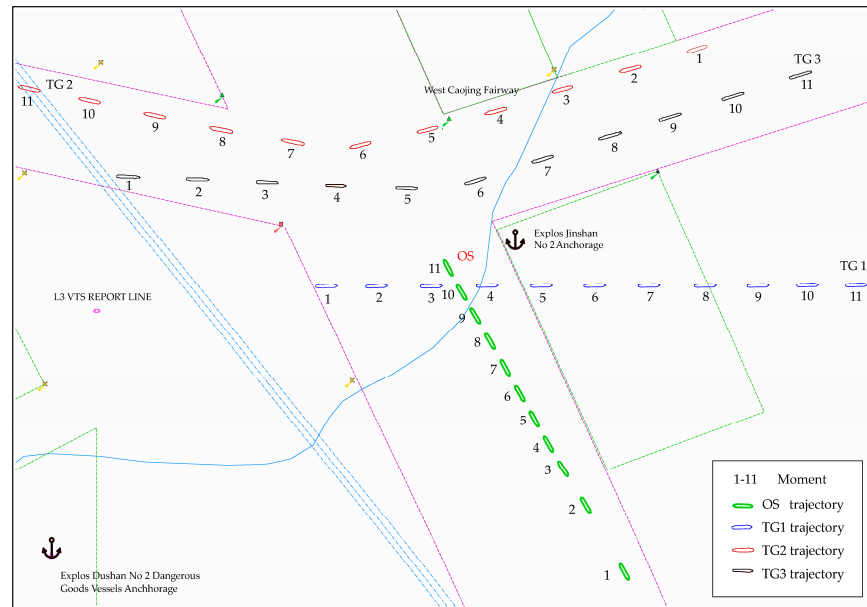


Figure 11. Simulation test on the motion trajectories of each vessel.

Figure 12 presents the curves of the d_{CPA} and t_{CPA} of each TG relative to OS over time. From the figure, it can be seen that, after driving for about 8 min under the given decision, the d_{CPA} values of OS and each TG are greater than 1 n miles. This indicates that the speed-varying collision avoidance measures for super-large vessels are highly feasible and in line with the “substantial” collision avoidance operation required in COLREGS.

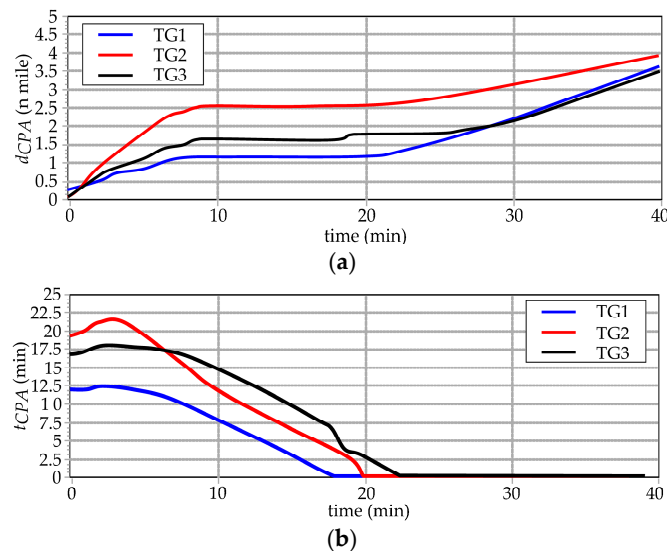


Figure 12. Changes in d_{CPA} and t_{CPA} values of the simulation test vessel. (a) The change of d_{CPA} value; (b) The change of t_{CPA} value.

6. Conclusions

In this paper, a CIPSO-based speed-varying collision avoidance decision support method is proposed for super-large vessel navigation in port waters. Focusing on the maneuvering characteristics of super-large vessels and the special characteristics of port waters, a vessel CRI sub-model is established, which takes the vessel domain and maneuvering performance into account, and the real-time CRI can be calculated to evaluate the safety of navigation. The speed-varying energy loss sub-model is constructed by limiting the range of decision values according to COLGERS. The two sub-models are weighted and combined to derive the total objective function for vessels' speed-varying collision avoidance, which is used as the fitness of CIPSO. A safety and effectiveness collision avoidance decision value can be derived through the iterative optimization process of CIPSO. Finally, a simulation analysis was performed based on numerical simulation and the simulator platform, and the simulation results demonstrate that the speed-varying collision avoidance method is suitable for the port waters. The performance of the CIPSO is compared with three well-established intelligent algorithms. The results indicate that the CIPSO exhibits a faster convergence, higher accuracy, and shorter iteration times when obtaining the optimal decision value. In addition, the feasibility and effectiveness of the proposed method are validated through the examination of the CRI, safe encounter distance, and simulator experiments.

The method can provide decision support for the navigation of super-large vessels in the port. It assumes compliance with COLREGS by all vessels. However, it is important to acknowledge that in real multi-vessel encounter situations, there is a possibility of human error or uncoordinated collision avoidance measures between vessels. Therefore, future work should further consider the existence of vessels that do not comply with COLREGS and set up scenarios in which vessels encounter uncoordinated collision avoidance operations.

Author Contributions: Conceptualization, B.X. and Y.Z.; methodology, Y.Z.; validation, B.X.; formal analysis, B.X.; investigation, Y.Z.; resources, Y.Z.; data curation, B.X.; writing—original draft preparation, B.X.; writing—review and editing, B.X. and Y.Z.; funding acquisition, Y.Z. All authors have read and agreed to the published version of the manuscript.

Funding: This research was partially funded and supported by National Natural Science Foundation of China grant number 52171346, Educational Science Planning Project of Guangdong Province grant number 2022KTSCX102.

Institutional Review Board Statement: Not applicable.

Informed Consent Statement: Informed consent was obtained from all subjects involved in the study.

Data Availability Statement: Not applicable.

Acknowledgments: The authors would like to thank Zhejiang Ocean University and Guangzhou Maritime University for their support.

Conflicts of Interest: The authors declare no conflict of interest.

References

1. Tadros, M.; Ventura, M.; Soares, C.G. Review of Current Regulations, Available Technologies, and Future Trends in the Green Shipping Industry. *Ocean Eng.* **2023**, *280*, 114670.
2. Paulauskas, V.; Filina-Dawidowicz, L.; Paulauskas, D. Navigation Safety on Shipping Routes during Construction. *Appl. Sci.* **2023**, *13*, 8593.
3. Lyu, H.; Hao, Z.; Li, J.; Li, G.; Sun, X.; Zhang, G.; Yin, Y.; Zhao, Y.; Zhang, L. Ship Autonomous Collision-Avoidance Strategies—A Comprehensive Review. *J. Mar. Sci. Eng.* **2023**, *11*, 830.
4. Sohail, A. Genetic Algorithms in the Fields of Artificial Intelligence and Data Sciences. *Ann. Data Sci.* **2023**, *10*, 1007–1018. [[CrossRef](#)]
5. Jwo, D.-J.; Biswal, A.; Mir, I.A. Artificial Neural Networks for Navigation Systems: A Review of Recent Research. *Appl. Sci.* **2023**, *13*, 4475.
6. Zhang, Y.; Zhang, D.; Jiang, H. A Review of Artificial Intelligence-Based Optimization Applications in Traditional Active Maritime Collision Avoidance. *Sustainability* **2023**, *15*, 13384.

7. Nayak, J.; Swapnarekha, H.; Naik, B.; Dhiman, G.; Vimal, S. 25 Years of Particle Swarm Optimization: Flourishing Voyage of Two Decades. *Arch. Comput. Methods Eng.* **2022**, *30*, 1663–1725.
8. Tsou, M.C.; Kao, S.L.; Su, C.M. Decision Support from Genetic Algorithms for Ship Collision Avoidance Route Planning and Alerts. *J. Navig.* **2010**, *63*, 167–182. [[CrossRef](#)]
9. Tsou, M.C. Multi-Target Collision Avoidance Route Planning under an ECDIS Framework. *Ocean Eng.* **2016**, *121*, 268–278. [[CrossRef](#)]
10. Fiskin, R.; Atik, O.; Kisi, H.; Nasibov, E.; Johansen, T.A. Fuzzy Domain and Meta-Heuristic Algorithm-Based Collision Avoidance Control for Ships: Experimental Validation in Virtual and Real Environment. *Ocean Eng.* **2021**, *220*, 108502.
11. Ni, S.; Liu, Z.; Cai, Y. Ship Manoeuvrability-Based Simulation for Ship Navigation in Collision Situations. *J. Mar. Sci. Eng.* **2019**, *7*, 90. [[CrossRef](#)]
12. Alvarez, A.; Caiti, A.; Onken, R. Evolutionary Path Planning for Autonomous Underwater Vehicles in a Variable Ocean. *IEEE J. Ocean Eng.* **2004**, *29*, 418–429. [[CrossRef](#)]
13. Lazarowska, A. Ship's Trajectory Planning for Collision Avoidance at Sea Based on Ant Colony Optimisation. *J. Navig.* **2015**, *68*, 291–307. [[CrossRef](#)]
14. Lazarowska, A. Multi-Criteria ACO-Based Algorithm for the Ship's Trajectory Planning. *TransNav J.* **2017**, *11*, 31–36. [[CrossRef](#)]
15. Tsou, M.C.; Hsueh, C.K. The Study of Ship Collision Avoidance Route Planning by Ant Colony Algorithm. *J. Mar. Sci. Technol.* **2010**, *18*, 18–22. [[CrossRef](#)]
16. Wang, S.; Huang, M.; Chen, C.; Sun, J.; Ma, F. A Path Planning Method for Ship Collision Avoidance Considering Spatial–Temporal Interaction Effects. *Appl. Sci.* **2022**, *12*, 5036. [[CrossRef](#)]
17. Lyu, H.; Yin, Y. Fast Path Planning for Autonomous Ships in Restricted Waters. *Appl. Sci.* **2018**, *8*, 2592. [[CrossRef](#)]
18. Shen, H.Q.; Hashimoto, H.; Matsuda, A.; Taniguchi, Y.; Terada, D.; Guo, C. Automatic Collision Avoidance of Multiple Ships Based on Deep Q-Learning. *Appl. Ocean Res.* **2019**, *86*, 268–288. [[CrossRef](#)]
19. Hu, L.; Naeem, W.; Rajabally, E.; Watson, G.; Mills, T.; Bhuiyan, Z.; Salter, I. COLREGs-Compliant Path Planning for Autonomous Surface Vehicles: A Multiobjective Optimization Approach. *IFAC-PapersOnLine* **2017**, *50*, 13662–13667. [[CrossRef](#)]
20. Xia, G.; Han, Z.; Zhao, B.; Wang, X. Local Path Planning for Unmanned Surface Vehicle Collision Avoidance Based on Modified Quantum Particle Swarm Optimization. *Complexity* **2020**, *2020*, 3095426. [[CrossRef](#)]
21. Ma, Y.; Hu, M.; Yan, X. Multi-Objective Path Planning for Unmanned Surface Vehicle with Currents Effects. *ISA Trans.* **2018**, *75*, 137–156. [[PubMed](#)]
22. Zheng, Y.; Zhang, X.; Shang, Z.; Guo, S.; Du, Y. A Decision-Making Method for Ship Collision Avoidance Based on Improved Cultural Particle Swarm. *J. Adv. Transp.* **2021**, *2021*, 1–31. [[CrossRef](#)]
23. Piotrowski, A.P.; Napiorkowski, J.J.; Piotrowska, A.E. Partical Swarm Optimization or Differential Evolution—A Comparison. *Eng. Appl. Artif. Intell.* **2023**, *121*, 106008.
24. Xie, S.; Chu, X.; Zheng, M.; Liu, C.G. Ship Predictive Collision Avoidance Method Based on an Improved Beetle Antennae Search Algorithm. *Ocean Eng.* **2019**, *192*, 106542.
25. Xu, Q.Y. Collision Avoidance Strategy Optimization Based on Danger Immune Algorithm. *Comput. Ind. Eng.* **2014**, *76*, 268–279. [[CrossRef](#)]
26. Wei, Z.K.; Zhao, K.; Wei, M. Decision-Making in Ship Collision Avoidance Based on Cat-Warm Biological Algorithm. In Proceedings of the 2015 International Conference on Computational Science and Engineering, Porto, Portugal, 21–23 October 2015; Atlantis: Amsterdam, The Netherlands, 2015; pp. 114–122.
27. Zhao, Y.L. *Collision Avoidance and Watch Keeping*; Dalian Maritime University Press: Dalian, China, 2010.
28. Liu, H.D.; Liu, Q.; Sun, R. Deterministic Vessel Automatic Collision Avoidance Strategy Evaluation Modeling. *Int. Autom. Soft Co.* **2019**, *25*, 789–804. [[CrossRef](#)]
29. Zhou, W.; Zheng, J.; Xiao, Y.J. An Online Identification Approach for Ship Domain Model Based on AIS Data. *PLoS ONE* **2022**, *17*, e0265266.
30. Li, Y.S.; Guo, Z.Q.; Yang, J.; Fang, H.; Hu, Y.W. Prediction of Ship Collision Risk Based on CART. *IET Intell. Transp. Syst.* **2018**, *12*, 1345–1350. [[CrossRef](#)]
31. Chen, S.; Ahmad, R.; Lee, B.G.; Kim, D. Composition Ship Collision Risk Based on Fuzzy Theory. *J. Cent. South Univ.* **2014**, *21*, 4296–4302. [[CrossRef](#)]
32. Szlapczynski, R.; Szlapczynska, J. Review of Ship Safety Domains: Models and Applications. *Ocean Eng.* **2017**, *145*, 277–289. [[CrossRef](#)]
33. Fujii, Y.; Tanaka, K. Traffic Capacity. *J. Navig.* **1971**, *24*, 543–552. [[CrossRef](#)]
34. Goodwin, E.M. A Statistical Study of Ship Domains. *J. Navig.* **1975**, *28*, 328–344. [[CrossRef](#)]
35. Davis, P.V.; Dove, M.J.; Stockel, C.T. A Computer Simulation of Marine Traffic Using Domains and Arenas. *J. Navig.* **1980**, *33*, 215–222. [[CrossRef](#)]
36. Coldwell, T.G. Marine Traffic Behaviour in Restricted Waters. *J. Navig.* **1983**, *36*, 430–444. [[CrossRef](#)]
37. Kijima, K.; Furukawa, Y. Automatic Collision Avoidance System Using the Concept of Blocking Area. *IFAC Proc. Vols.* **2003**, *36*, 223–228. [[CrossRef](#)]
38. Pietrzykowski, Z.; Uriasz, J. The Ship Domain—A Criterion of Navigational Safety Assessment in an Open Sea Area. *J. Navig.* **2009**, *62*, 93–108. [[CrossRef](#)]

39. Wang, N.; Meng, X.; Xu, Q.; Wang, Z. A Unified Analytical Framework for Ship Domains. *J. Navig.* **2009**, *62*, 643–655.
40. Venkateswaran, C.; Ramachandran, M.; Ramu, K.; Prasanth, V.; Mathivanan, G. Application of Simulated Annealing in Various Field. *Mater. Its Charact.* **2022**, *1*, 100299. [[CrossRef](#)]
41. Alhijawi, B.; Awajan, A. Genetic Algorithms: Theory, Genetic Operators, Solutions, and Applications. In *Evolutionary Intelligence*; Springer: Berlin/Heidelberg, Germany, 2023; pp. 1–12.
42. Shami, T.M.; El-Saleh, A.A.; Alswaitti, M.; Al-Tashi, Q.; Summakieh, M.A.; Mirjalili, S. Particle Swarm Optimization: A Comprehensive Survey. *IEEE Access* **2022**, *10*, 10031–10061. [[CrossRef](#)]

Disclaimer/Publisher’s Note: The statements, opinions and data contained in all publications are solely those of the individual author(s) and contributor(s) and not of MDPI and/or the editor(s). MDPI and/or the editor(s) disclaim responsibility for any injury to people or property resulting from any ideas, methods, instructions or products referred to in the content.